Inverse Optimal Design of the Radiant Heating in Materials Processing and Manufacturing

A.G. Fedorov, K.H. Lee, and R. Viskanta

(Submitted 13 April 1998; in revised form 5 August 1998)

Combined convective, conductive, and radiative heat transfer is analyzed during heating of a continuously moving load in the industrial radiant oven. A transient, quasi-three-dimensional model of heat transfer between a continuous load of parts moving inside an oven on a conveyor belt at a constant speed and an array of radiant heaters/burners placed inside the furnace enclosure is developed. The model accounts for radiative exchange between the heaters and the load, heat conduction in the load, and convective heat transfer between the moving load and oven environment. The thermal model developed has been used to construct a general framework for an inverse optimal design of an industrial oven as an example. In particular, the procedure based on the Levenberg-Marquardt nonlinear least squares optimization algorithm has been developed to obtain the optimal temperatures of the heaters/burners that need to be specified to achieve a prescribed temperature distribution of the surface of a load. The results of calculations for several sample cases are reported to illustrate the capabilities of the procedure developed for the optimal inverse design of an industrial radiant oven.

Keywords heat transfer, inverse design, materials processing, optimization design, radiant heating

1. Introduction

In many materials processing applications such as drying of paper, thermal finishing of coating, and others, a procedure frequently encountered involves material moving continuously inside an oven while being heated (Ref 1). As an example, an infrared radiant oven typically consists of the array of heaters/burners placed on the top, bottom, and sometimes the sides of the enclosure. Electrical resistance or gas-fired heaters are used to heat the material to a desired temperature. The heaters/burners provide a steady supply of the thermal radiation to the load as it moves inside the oven.

The problem considered in this paper is concerned with an inverse design of the oven capable of providing the optimal conditions for thermal treatment of the load. The technical issue is to determine the design and operating parameters of the oven (temperatures of each heater/burner, size of the heaters, etc.) that satisfy the optimal performance criteria prescribed by the user (specific temperature distribution on the surface of the moving load or heating uniformity, energy efficiency, and others).

This article describes a transient, quasi-three-dimensional model of heat transfer in the radiant heating oven coupled to the load moving inside the oven as the material is thermally treated. The model considers radiation exchange between the heaters and the load, heat conduction in the load, and convective heat transfer between a moving load and gaseous oven environment. The thermal model developed is then combined with the Levenberg-Marquardt nonlinear least squares optimization algorithm to find the optimal temperatures of each heater/burner and other operating parameters that produce an arbitrary but physically realistic temperature distribution on the surface of a load as prescribed by the process designer/operator. This inverse design procedure is applied to several sample cases to illustrate the potential capabilities of the approach.

A.G. Fedorov, K.H. Lee, and **R. Viskanta,** Heat Transfer Laboratory, School of Mechanical Engineering, Purdue University, West Lafayette, IN 47907, USA. Contact e-mail: viskanta@ecn.purdue.edu.

2. Thermal Model Description

2.1 General Problem Formulation

Consider an industrial oven to be the parallelepiped enclosure formed by the six walls of refractories or other insulating materials capable of withstanding the high temperature environment (see Fig. 1). The continuously moving strip of material or stock placed on the conveyor belt progresses through the furnace while being thermally treated. In general, the opaque load could be virtually of any shape, and an arrangement of the heaters inside the furnace could also be arbitrary.

The load is heated while being transported in a horizontal plane. Heat transfer to the surface of the moving load is by

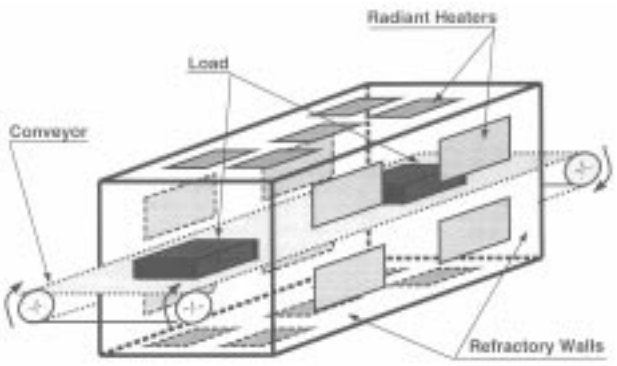

Fig. 1 Schematic diagram of an industrial radiant oven

combined radiation and convection. The infrared heaters supply radiant energy to the material. The moving strip or belt and buoyancy due to the large temperature gradients between the heaters, oven walls, and load induce an exceedingly complex flow of the gas inside the oven. This results in the mixed convection heat transfer from the gas to the load surface. In the load, the thermal energy storage, conduction, advection, and possible phase transformations (melting of coating, evaporation, and chemical reactions) must be considered.

Different modes of heat transfer occurring in the furnace are illustrated schematically in Fig. 2. The instantaneous heat flux at any point (s) on the load surface includes contributions due to radiation exchange between heaters and the load and between refractories and the load (q^r_{lh} and q^r_{lw}, respectively), convection to the gaseous environment (q^c_{lg}), and possible phase transformation (q^t) (Fig. 2) and can be written as:

$$q(s) = q^r_{lh}(s) + q^r_{lw}(s) + q^c_{lg}(s) + q^t(s) \qquad \text{(Eq 1)}$$

Equation 1 is to be used in the overall dynamic thermal model as the boundary condition at the load surface at every time instant.

The final step of the inverse optimal design is integration of the thermal model of the furnace enclosure and load dynamics into a suitable optimization algorithm. The general optimization procedure and the information flow in the optimal design algorithm are illustrated in Fig. 3.

Apparently, the general furnace geometry and heat transfer processes occurring in the oven are very complex and, hence, must be simplified for the purpose of mathematical analysis.

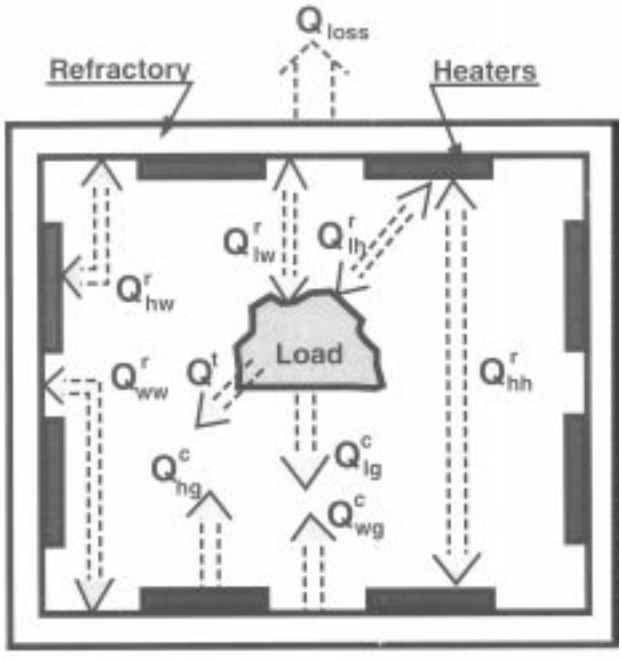

Fig. 2 Schematic illustrating modes of heat transfer in an industrial oven (superscripts *r*, *c*, and *t* refer to radiation, convection, and phase transformation, respectively: subscripts *l*, *w*, *h*, and *g* refer to load, refractory wall, heater, and gas, respectively)

The next section describes a mathematical model of radiative heating of the load in an oven of a simple design with flat heaters placed only on the roof and the floor of the unit. Of course, the model easily could be extended to include a case when heaters are placed on the side and end walls of the oven enclosure.

2.2 Simplified Problem: Model Equations

A schematic diagram of an industrial oven of a simple design for radiant heating of the load moving at a constant velocity U_0 together with the coordinate system is shown in Fig. 4.

The radiant heaters are placed only on the top and the hearth, while the load (a thin rectangular sheet of the material) is moving in the middle of the oven. The heaters are assumed to be flat and kept at the uniform temperature although different in the absolute value for each individual heater. A particular geometrical arrangement of the heater arrays will be given with the results of sample calculations. Note that due to a symmetry of the system, only the upper part of the entire arrangement is shown in Fig. 4.

To simplify the problem, it is assumed that radiation heat transfer occurs only between the heaters and the surface of the load. The radiation incident on the refractory walls, which is reflected toward the load surface, is assumed to be negligibly small in comparison to the direct radiation exchange between the heaters and the load.

Also, it is assumed that the gases filling the oven enclosure are radiatively nonparticipating. Radiation and convection are considered as two independent heat transfer modes that are acting in parallel. Doing this renders the interaction between convective and radiative heat transfer at all surfaces including that of the load (Ref 2), negligible. Furthermore, in order to calculate the convective heat transfer from the oven gas to the load, the oven gas temperature (T_g) and the convective heat transfer coefficient (h_g) are taken to be constant. The convective coefficient is calculated from an empirical correlation given by

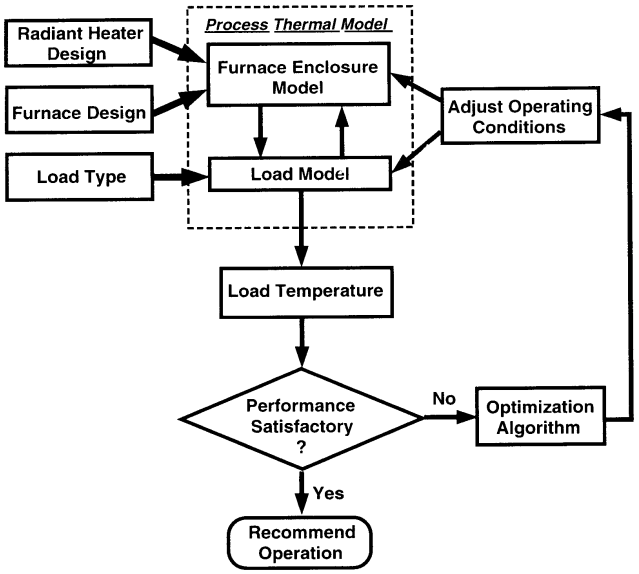

Fig. 3 Model structure and optimization procedure information flow

Incropera and DeWitt (Ref 3). Additional assumptions which allow simplification in the mathematical treatment of the process are given.

Finally, in this particular example we do not consider thermal effects associated with possible phase transformation and/or chemical reactions occurring in the material or at the surface. However, those effects, if present, could be included readily in the mathematical model in a straightforward fashion.

An industrial oven as shown in Fig. 4 is a three-dimensional system. However, for simplicity of analysis, the following coordinate decomposition is applied: first, the radiation heat exchange problem is formulated and solved considering the heaters and the load surface in the *x*-*z* plane only; then, the load material is divided into rectangular parallel elements along the *z* direction, and the transient advection-conduction heat transfer problem is solved for each (x-*y*) strip of the load separately. Such a decomposition is implicitly based on the assumption that the temperature gradient in the material along the *z* direction is much smaller than those along *x* and *y* directions and, hence, can be safely ignored. Given above, the energy equation for each (*x*-*y*) strip of the load (*z* is fixed) can be written as:

$$\frac{\partial (\rho cT)}{\partial t} + U_0 \frac{\partial (\rho cT)}{\partial x} = \frac{\partial}{\partial x}\left[k \frac{\partial T}{\partial x}\right] + \frac{\partial}{\partial y}\left[k \frac{\partial T}{\partial y}\right] \quad \text{for each } 0 \le z \le W \tag{Eq 2}$$

Note that in the present formulation, the thermophysical properties (density ρ, specific heat *c*, and thermal conductivity *k*) of the load material can be given as direction dependent.

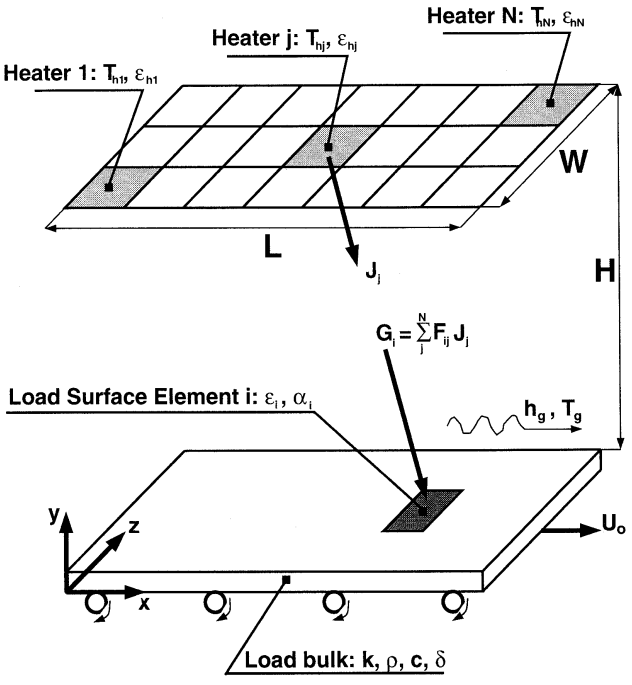

Fig. 4 Schematic of the physical arrangement and the coordinate system

The initial transient heating of the load is considered to be very short compared to the time it takes the load to traverse the heated length *L* and is, therefore, neglected ($\partial T/\partial t \to 0$). This assumption together with the relationship $x = Vt$ allows Eq 2 to be written in the following form:

$$U_0 \frac{\partial (\rho cT)}{\partial x} = \frac{\partial}{\partial x}\left[k \frac{\partial T}{\partial x}\right] + \frac{\partial}{\partial y}\left[k \frac{\partial T}{\partial y}\right] \quad \text{for each } 0 \le z \le W \tag{Eq 3}$$

To conclude the mathematical formulation of the problem we need to provide the appropriate boundary conditions. In particular, the load temperature at the inlet to the oven $x = 0$ is equal to the initial "cold" load temperature, $T(0, y, z) = T_{in}$, and the temperature gradient along the *x* direction is assumed to vanish at the exit of the oven, that is, $\partial T(L, y, z)/\partial x = 0$. As indicated above, the heat transfer at the upper and lower horizontal load surfaces is by combined radiation and convection and can be stated as:

$$-k \frac{\partial T}{\partial y} = \int_0^\infty q_\lambda^r d\lambda + h_g [T_g - T(x, z)] \text{ at } y = 0 \tag{Eq 4}$$

$$k \frac{\partial T}{\partial y} = \int_0^\infty q_\lambda^r d\lambda + h_g [T_g - T(x, z)] \text{ at } y = \delta \tag{Eq 5}$$

The model for calculating the radiative heat fluxes q^r is detailed in the following subsection.

2.3 Radiation Heat Exchange

It is clear from Eq 4 and 5 that the model takes into account spectral dependence of radiation in calculating the total net radiative fluxes at the load surface. Specifically, all surfaces (that is, those of heaters and of the load) are assumed to be diffuse absorbers and reflectors of radiation, and the integration over the entire wavelength spectrum (from 0 to ∞) is carried out using band models. To this end, the entire wavelength region is divided into a finite number of bands, N_b, such that:

$$\int_0^\infty q_\lambda^r d\lambda = \sum_{k=1}^{N_b} \left\{ \alpha_{\Delta\lambda_k} G^k(x, z) \Delta\lambda_k - \varepsilon_{\Delta\lambda_k} E_b(T) [f(\lambda_{k+1} T) - f(\lambda_k T)] \right\} \tag{Eq 6}$$

Equation 6 requires the band-averaged spectral radiation properties $\varepsilon_{\Delta\lambda_k}$ and $\alpha_{\Delta\lambda_k}$, the expression for the fractional spectral black body emitted flux $f(\lambda_k T)$, and a model for the spectral irradiation to the load G^k. The radiation properties of the load material can be found in the literature or must be obtained through direct experimentation.

The fractional spectral black body emitted flux $f(\lambda_k T)$ is given by the integral (Ref 4):

$$f(\lambda_k T) = \int_0^{\lambda_k T} E_{b\lambda}(T) d\lambda / E_b(T) \quad \text{(Eq 7)}$$

with the spectral and total black body emitted fluxes defined as:

$$E_{b\lambda}(T) = 2C_1 / \lambda^5 \, [exp(C_2 / \lambda T) - 1] \quad \text{(Eq 8)}$$

and

$$E_b(T) = \int_0^{\infty} E_{b\lambda}(T) d\lambda = \sigma T^4 \quad \text{(Eq 9)}$$

respectively. The constants C_1 and C_2 are equal to 0.59548×10^{-16} W m^2 and 1.43879 cm K, respectively, and σ ($=5.670 \times 10^{-8}$W/m^{2}K) is the Stefan-Boltzmann constant.

Since the load and the oven walls are assumed to be "cold" compared to the heaters, the problem is generally simplified and the radiation heat exchange between the heaters and the load surfaces is no longer coupled. In particular, the irradiation on the load surface element, *i*, (Fig. 4) for wavelength band $\Delta\lambda_k$ can be expressed as:

$$G_i^k = \sum_{j=1}^{N_h} F_{ij} J_j^k \quad \text{(Eq 10)}$$

where N_h is the total number of heaters on one side only (top or bottom) and F_{ij} are the configuration (view angle) factors which are determined from the layout of the heater, *j*, with respect to the *i*th load surface element (Ref 4). For the geometry considered, these factors are given by Hsu (Ref 5). Lastly, the radiosity J_j^k or leaving flux from the *j*th heater in the wavelength interval $\Delta\lambda_k = \lambda_{k+1} - \lambda_k$ is given by:

$$J_j^k = \varepsilon_j^h \, E_b(T_{hj}) \, [f(\lambda_{k+1} T_{hj}) - f(\lambda_k T_{hj})] \quad \text{(Eq 11)}$$

where ε_j^h stands for the emissivity of the *j*th heater and the total and fractional spectral black body emitted fluxes $E_b(T_{hj})$ and $f(\lambda_k T_{hj})$ for band $\Delta\lambda_k$ can be computed from Eq 9 and 7, respectively, for a given temperature of the heater T_{hj}. For the sake of completeness, it should be mentioned that the general formulation of the problem which includes radiation exchange between all components of the industrial oven is available (Ref 6).

2.4 Method of Solution

Clearly, given the geometry (size and location) and temperature for each heater and the thermophysical and radiative properties of the load and heaters as the input information, one can readily calculate total and fractional spectral black body emitted fluxes $E_b(T_{hj})$ and $f(\lambda_k T_{hj})$ for each band $\Delta\lambda_k$ of the entire spectrum, the configuration factors F_{ij}, radiosity J_j^k, and, in turn, the irradiation G_i^k. This completes the formulation of boundary conditions, Eq 4 and 5, and, hence, the energy conservation Eq 3 can be solved for each (*x*-*y*) strip at *z* = const.

Equation 3 is of the elliptic type and can be solved using the finite volume numerical integration technique described by Patankar (Ref 7). Suffice it to mention that each *x*-*y* strip is subdivided into finite rectangular volumes over which the energy conservation equation is integrated using the finite-difference approximation for spatial derivatives and then solved iteratively by the tridiagonal matrix inversion algorithm. The temperature is underrelaxed by factor of 0.5 in order to achieve the stable converged solution.

The numerical algorithm can be summarized in the steps:

1. Read geometric and operating data.
2. Initialize variables and set up the numerical grid in the load.
3. Compute the configuration factors.
4. Compute the irradiation and emitted fluxes at the load surface elements.
5. Solve energy equation for each *x*-*y* element of the load.
6. Print out the resulting temperature and heat flux distributions.

3. Optimization Algorithm

3.1 Problem Formulation

As stated in the introduction, it is desirable to use the thermal model described in the previous section as an analytical tool for an intelligent thermal design of the radiantly heated industrial oven. For example, it is desirable to find an algorithm which allows one to find the temperatures of each separate heater such that an oven operator can obtain a prescribed spatial temperature distribution on the surface of the load being processed.

In general terms, the nonlinear least square optimization problem can be stated as: find the optimal values of the optimization variables $X = (x_1,\ldots,x_n)$ (for example, operating temperature of the heaters) which minimize the L^2-norm of a particular prescribed function $F(X) = (f_1,\ldots,f_m)$ (for example, the squared difference between achieved and prescribed temperatures at the load surface):

$$\min_{X \varepsilon R^n} \| F(X) \| = \min_{X \varepsilon R^n} \frac{1}{2} F(X)^T F(X) = \min_{X \varepsilon R^n} \frac{1}{2} \sum_{i=1}^{m} f_i(X)^2 \quad \text{(Eq 12)}$$

$$L \le X \le U \text{ or } l_j \le x_j \le u_j, \; j = 1,\ldots, n \quad \text{(Eq 13)}$$

Note that the number of points where *F* is evaluated (that is, *m*) must always be larger than number of optimization variables *X* (that is, *n*) for correct problem formulation. Equation 13 allows a user to set the simple bounds on each operating parameter (for

example, the heater temperature may be set not to exceed some given temperature recommended by the heater manufacturer).

3.2 Solution Algorithm

To solve the given optimization problem, Eq 12 and 13, a modified Levenberg-Marquardt iterative method (Ref 8, 9) is employed. Starting from the initial guess point X_0, the optimization routine builds the active set *IA* on every iteration which contains the variables x_j at their respective lower and upper bounds l_j and u_j. The variable x_j is called a free variable if it is not in the current active set *IA*. The algorithm then computes the search direction for the free variables in the next step according to the formula:

$$d = -(J^T J + \mu I)^{-1} J^T F(X) \quad \text{(Eq 14)}$$

where μ is the Levenberg-Marquardt parameter, I is a unitary matrix, and $J = J_{ij} = \partial f_i / \partial x_j$ is the Jacobian with respect to the free variables. The search direction for the variables in the active set *IA* is set to zero. Then, the trust region approach discussed by Dennis and Schnabel (Ref 10) is used to find the new point X. Finally, the optimality conditions are stated in the form:

$$||J(X^*)|| \le \varepsilon \text{ for } l_j < x_j^* < u_j,\ j = 1, \ldots, n \quad \text{(Eq 15)}$$

$$J(x_j^*) < 0 \text{ for } x_j^* = u_j,\ j = 1, \ldots, n \quad \text{(Eq 16)}$$

$$J(x_j^*) > 0 \text{ for } x_j^* = l_j,\ j = 1, \ldots, n \quad \text{(Eq 17)}$$

The process is iteratively repeated until the optimality criterion ($\varepsilon = 1 \times 10^{-5}$) is met.

3.3 Practical Implementation

The optimization algorithm described in the previous subsection is practically implemented using the numerical routines DBCLSF and DU4LSF from the International Mathematical and Statistical Libraries (IMSL). The computer routine which numerically solves the thermal model of the industrial oven is used to compute the values of the minimizing function $F(X)$ at each iteration and linked with DBCLSF and DU4LSF optimization routines in one general computer program.

It should be noted that the numerical computations involved in the described optimal design procedure can be extremely time demanding. Often, several days of continuous program running on the SUN workstation were needed in order to achieve an optimal solution of the problem.

4. Sample Calculations

This section of the paper describes the results of inverse optimal oven design for several concrete sample cases. The objective is to demonstrate the robustness and relevance of the optimization procedure developed to the real world design applications.

4.1 Sample Case 1

The heater arrangement for this simulation is shown in Fig. 5. Both surfaces of the moving load are exposed to 20 staggered and equal size heaters located on the crown and bottom of the furnace at the same distance H = 0.5 m from the moving stock. The length, L, and width, W, of the oven roof and hearth, taken to be the same as the dimensions of the load (Fig. 4), are equal to 4 and 2 m, respectively.

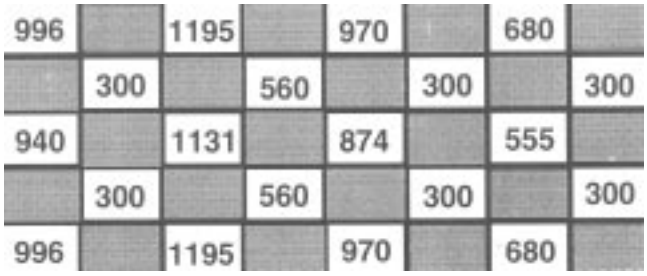

Fig. 5 Arrangement and operating temperatures (in degrees K) for the heaters (load velocity U_0 = 0.05 m/s)

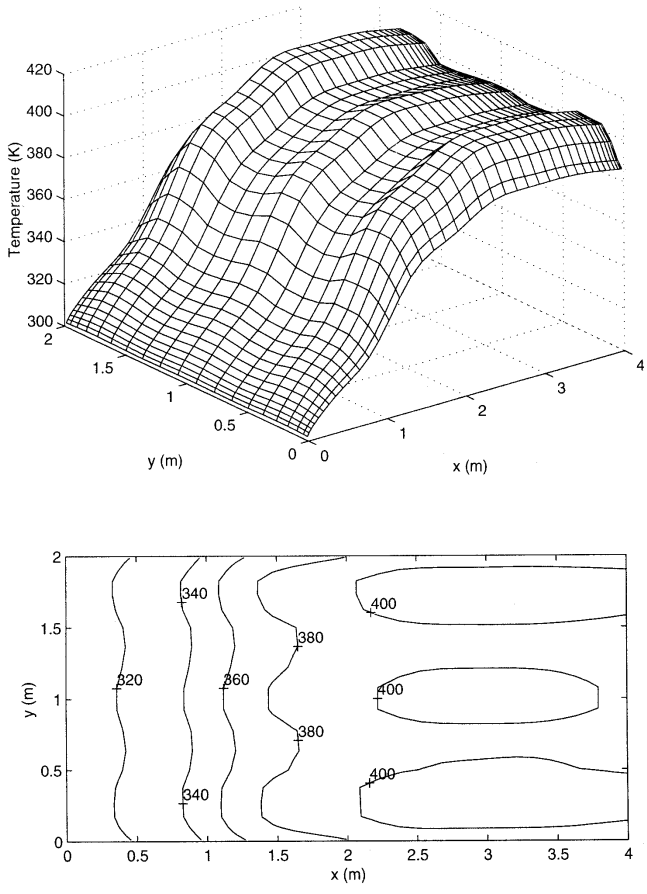

Fig. 6 Temperature distribution on the load surface (load velocity U_0 = 0.05 m/s)

The objective of the virtual design is to find the optimal operating temperatures for each heater T_{hj} such that the temperature field on the surface of the load approaches the prescribed function:

$$T_{\text{def}} = (1 - x) \times 300 + x \times 400 \text{ K if } 0 \le x \le 2 \text{ m} \quad \text{(Eq 18)}$$

$$T_{\text{def}} = 400 \text{ K if } 2 \text{ m} < x \le 4 \text{ m} \quad \text{(Eq 19)}$$

It is clear that the vector of optimization variables X consists of heater temperatures (that is, $x_j = T_{hj}$) and the function $F(X)$ to be minimized is simply given by the difference between the current and prescribed load surface temperatures at each grid node, i, [that is, $F = \{f_i\} = (T_{\text{current}} - T_{\text{def}})$]. Also imposed are the lower L and upper U limiting bounds on each heater temperature as equal to 300 K and 2000 K , respectively. This completes the formulation of the optimization problem as given by Eq 12 and 13.

All other operating and geometrical parameters are summarized:

- Thickness of the load $\delta = 0.002$ m
- Load velocity $U_0 = 0.05$ m/s
- Initial temperature of the load $T_{in} = 300$ K
- Emissivity $\varepsilon_{\Delta\lambda_k}$ and absorptivity $\alpha_{\Delta\lambda_k}$ of the load surface are taken to be the same for every band $\Delta\lambda_k$ and equal to 0.8 (that is, the gray approximation is used)
- Thermophysical properties of the load are: $\rho = 5000$ kg/m^3, $c = 1000$ J/kgK, and $k = 0.5$ W/mK
- Emissivity of the heaters $\varepsilon^h = 0.9$

The uniform grid on the load with 42 nodes in x direction and 22 nodes in both y and z directions is employed in the simulation in order to establish grid-independent and convergent solutions.

The optimized spatial distribution of the temperature, heat flux, and incident radiative flux on the load surface are shown in Fig. 6, 7, and 8, respectively. Clearly, the temperature distribution on the surface of the load, (Fig. 6) which resulted from application of the optimization procedure, matches very closely a prescribed temperature field as given in Eq 18 and 19. The values of the operating temperature for each heater, which produce such a temperature distribution, are found as a result of the optimization search and are presented in Fig. 5.

As follows from Fig. 5, the temperature of different heaters varies significantly and could hardly be anticipated from general physical considerations without an explicit mathematical

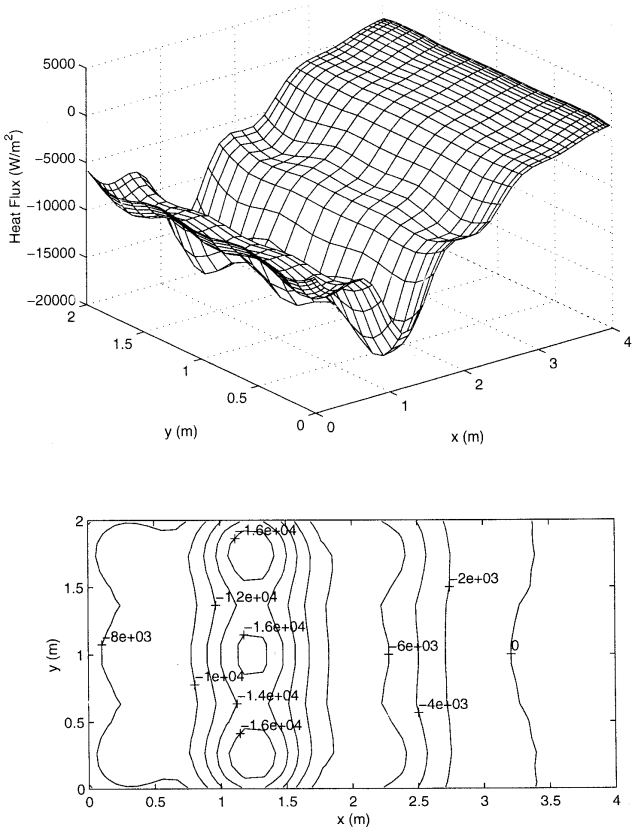

Fig. 7 Heat flux distribution on the load surface (load velocity $U_0 = 0.05$ m/s)

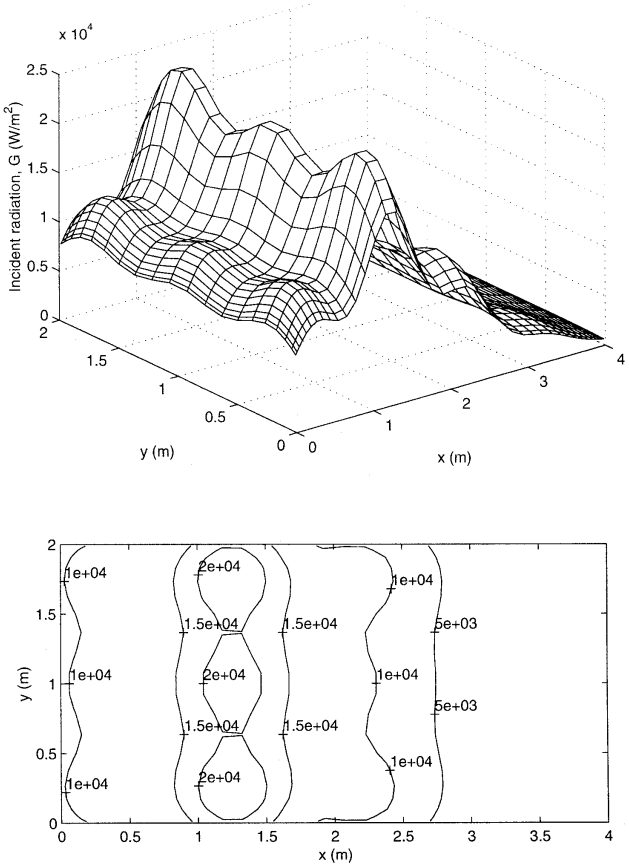

Fig. 8 Incident radiative flux distribution on the load surface (load velocity $U_0 = 0.05$ m/s)

optimization. Also, the optimization algorithm dictates that only 16 out of 20 heaters must be turned on to obtain a desired load surface temperature (the heaters having operating temperature 300 K can be viewed as simply being turned off).

4.2 Sample Case 2

This case is intended to illustrate the effect of the load velocity on the optimal operating temperatures of the radiant heaters. Hence, the optimization procedure is applied to the system (oven plus load) that is described by the same set of parameters as that in Case 1, but the load velocity is increased by a factor of two (that is, $U_0 = 2 \times 0.05 = 0.1$ m/s). The prescribed temperature distribution on the load surface is also the same as in Case 1 and is given by Eq 18 and 19.

Figures 9, 10, and 11 show the spatial distributions of the temperature, heat flux, and incident radiative flux on the load surface, respectively, as the results of the inverse optimal design. Again, as one can conclude from Fig. 9, the load surface temperature is virtually the same as that defined by Eq 18 and 19. The set of optimal operating temperatures for each heater that leads to the prescribed load surface temperature is presented in Fig. 12. As expected, these temperatures are higher than those obtained in the previous case because the residence time for the load in the oven decreases with an increase in the load (conveyor) velocity. As a result, higher energy input and, consequently, higher heater temperatures are required to bring the load surface temperature to the desired condition. However, it should be noted that despite a two-fold decrease in the residence time, the optimal temperatures of the heaters increase by only a few percent due to nonlinear dependence of the radiative heat flux on the temperature.

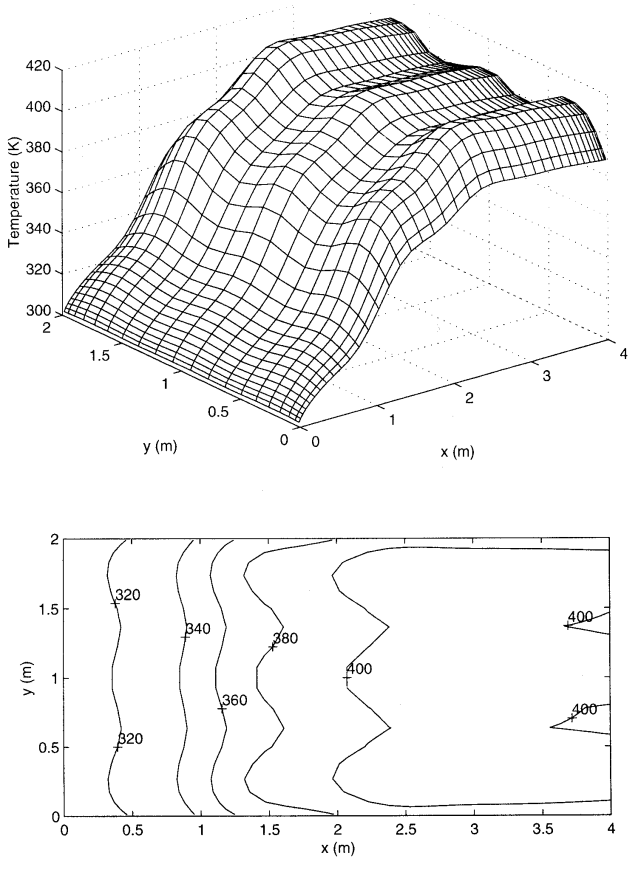

Fig. 9 Temperature distribution on the load surface (load velocity $U_0 = 0.1$ m/s)

5. Conclusions

This paper presents a formulation of an inverse design problem and solution algorithm of the radiant heating in an industrial oven for material processing applications. Two sample simulations have been analyzed, and the results of calculations lead to the conclusions:

- The use of the optimization technique in conjunction with a detailed thermal model for the radiant heating process appears to be a very powerful analytical approach that allows the system designer and/or operator to identify the optimal values of the operating furnace parameters. In general, almost every operating parameter (for example, speed of the load, size, number, and location of heaters, etc.) can be included into an optimization loop, which, in turn, can be constrained by almost any conditional bounds (for example, lower limit on thermal efficiency of the heaters, upper limit on fuel consumption, and others).
- A traditional forward design approach involves multiple trials and, hence, can be used only for very simple systems and processes where the forward search is guided by the intuition of the designer. In more general settings, when the system geometry is complex and multiple modes of transport processes are present, the use of the formal and mathematically sound optimization algorithms is highly desirable.
- Inverse optimal design is a numerically intensive technique that often requires large computer resources to address the problem in a timely fashion. However, continuous advances in computer technology and development of the novel optimization algorithms allow optimism about an increase in practical applications of the inverse optimization methods in the thermal engineering design and real time operation of the system.
- This paper has presented results of inverse optimal design of the heating process under three major simplifying assumptions: (a) the load is considered to be a thin sheet of material continuously moving inside the furnace, (b) the load surface and refractory walls are taken to be "cold" in comparison to the heaters in order to decouple the radiation exchange model, and (c) the oven contents (gases) are viewed as a nonparticipating medium. Hence, for other specific applications (for example, high temperature treatment of the discrete parts transported on the conveyer belt) the same methodology can still be applied but more complex thermal models will be needed. The analysis can also be extended to high-temperature furnaces where radiation heat transfer from the refractory walls to the load must be accounted for as has been done elsewhere (Ref 6).

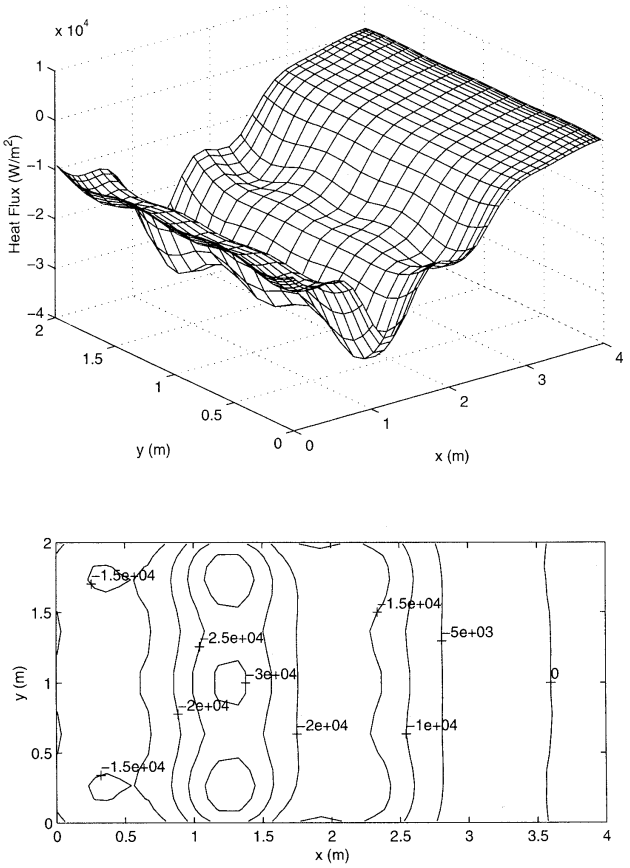

Fig. 10 Heat flux distribution on the load surface (load velocity U_0 = 0.1 m/s)

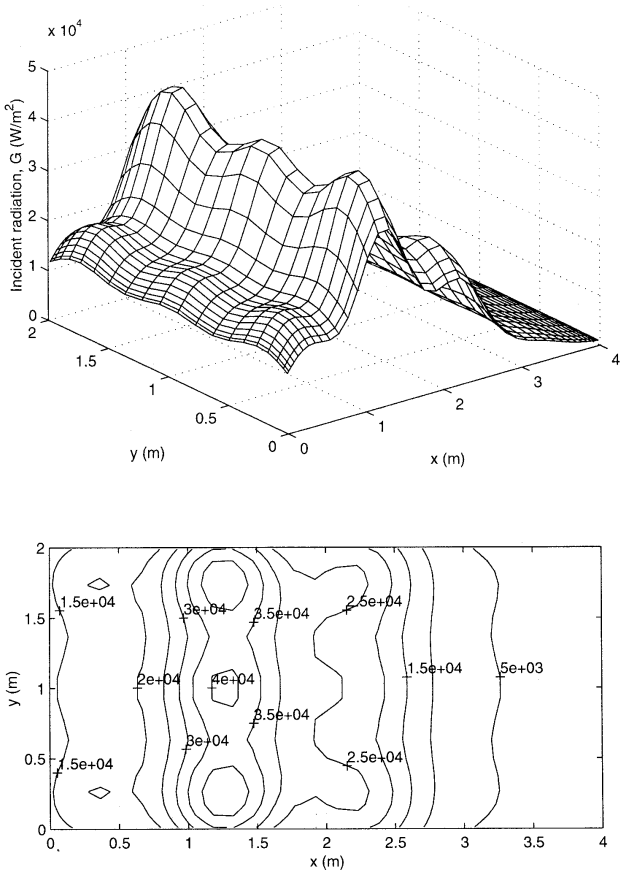

Fig. 11 Incident radiative flux distribution on the load surface (load velocity U_0 = 0.1 m/s)

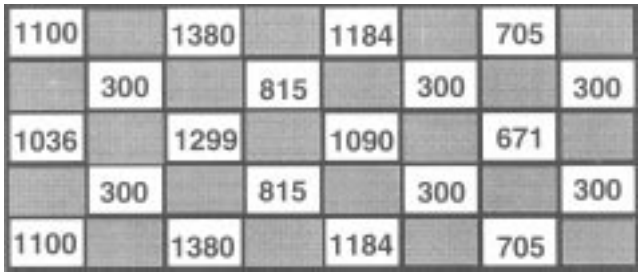

Fig. 12 Arrangement and operating temperatures (in degrees K) for the heaters (load velocity U_0 = 0.1 m/s)

References

1. R. Pritchard, J. Guy, and N. Conner, *Handbook of Industrial Gas Utilization*, Van Nostrand Reinhold Company, 1977
2. R.B. Mansour and R. Viskanta, Radiative and Convective Heat Transfer in Furnaces for Material Processing, *Proc. of the First International Conference on Transport Phenomena in Processing*, (Lancaster, PA), Technomic Publishing Co., Inc., 1992, p 693-713
3. F. Incropera and D. DeWitt, *Fundamentals of Heat and Mass Transfer*, Wiley, 1996
4. R. Siegel and J. Howell, *Thermal Radiation Heat Transfer*, McGraw-Hill, 1992
5. C.-J. Hsu, Shape Factor Equations for Radiant Heat Transfer Between Two Arbitrary Sizes of Rectangular Planes, *Can. J. of Chem. Eng.*, Vol 45, 1967, p 58-60
6. H. Yoshino and R. Viskanta, A Dynamic Thermal System Model for a Low Inertia Furnace, accepted for presentation and publication in Proc. of the 7th AIAA/ASME Thermophysics and Heat Transfer Conference, (Albuquerque, NM), 15-17 June 1998
7. S.V. Patankar, *Numerical Heat and Fluid Flow*, Hemisphere Publishing Corp., 1980
8. K. Levenberg, A Method for the Solution of Certain Problems in Least Squares, *Quarterly in Applied Mathematics*, Vol 2, 1944, p 164-168
9. D. Marquardt, An Algorithm for Least-Squares Estimation of Non-linear Parameters, *SIAM Journal of Applied Mathematics*, Vol. 11, 1963, p 431-441
10. J. Dennis and R. Schnabel, *Numerical Methods for Unconstrained Optimization and Nonlinear Equations*, Prentice-Hall, 1983